Science Advances
AAAS

advances.sciencemag.org/cgi/content/full/4/11/eaav2131/DC1

Supplementary Materials for

Mechanism of FACT removal from transcribed genes by anticancer drugs curaxins

Han-Wen Chang, Maria E. Valieva, Alfiya Safina, Răzvan V. Chereji, Jianmin Wang, Olga I. Kulaeva, Alexandre V. Morozov, Mikhail P. Kirpichnikov, Alexey V. Feofanov, Katerina V. Gurova, Vasily M. Studitsky*

*Corresponding author. Email: vasily.studitsky@fccc.edu

Published 7 November 2018, *Sci. Adv.* **4**, eaav2131 (2018)
DOI: 10.1126/sciadv.aav2131

This PDF file includes:

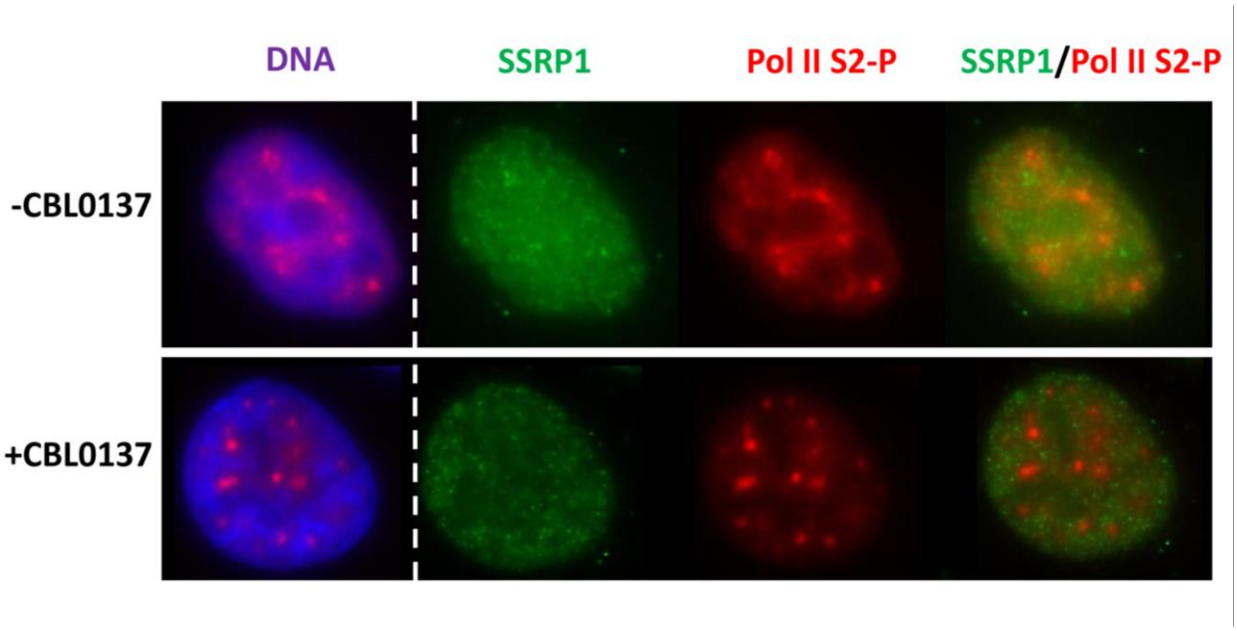

Fig. S1. Analysis of colocalization of FACT and transcribing Pol II using immunofluorescence. HT1080 cells were incubated in the presence of 3 uM CBL0137 for 4 hours. Then cells were fixed and stained with the indicated antibodies and Hoechst 33342 (DNA).

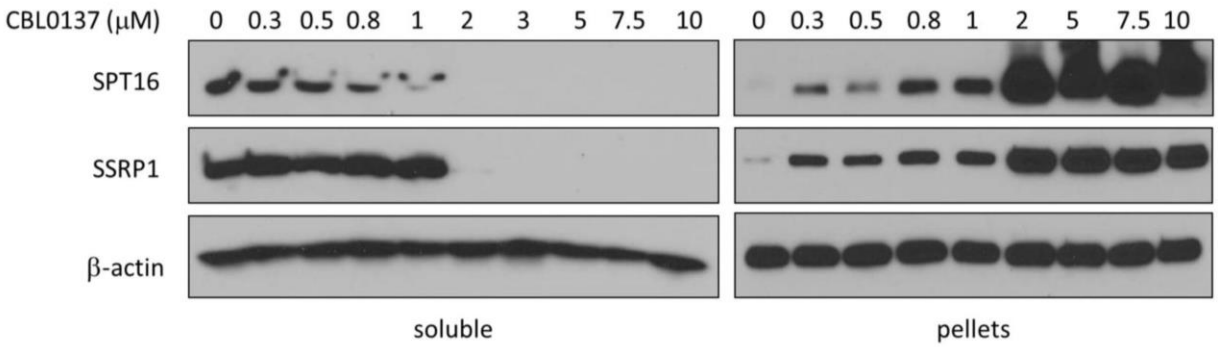

Fig. S2. Redistribution of FACT in HT1080 cells from nucleoplasm to chromatin. Immunoblotting of soluble and insoluble (pellets) fractions of cell nuclear extracts after treatment with different concentrations of CBL0137 for 1 hour.

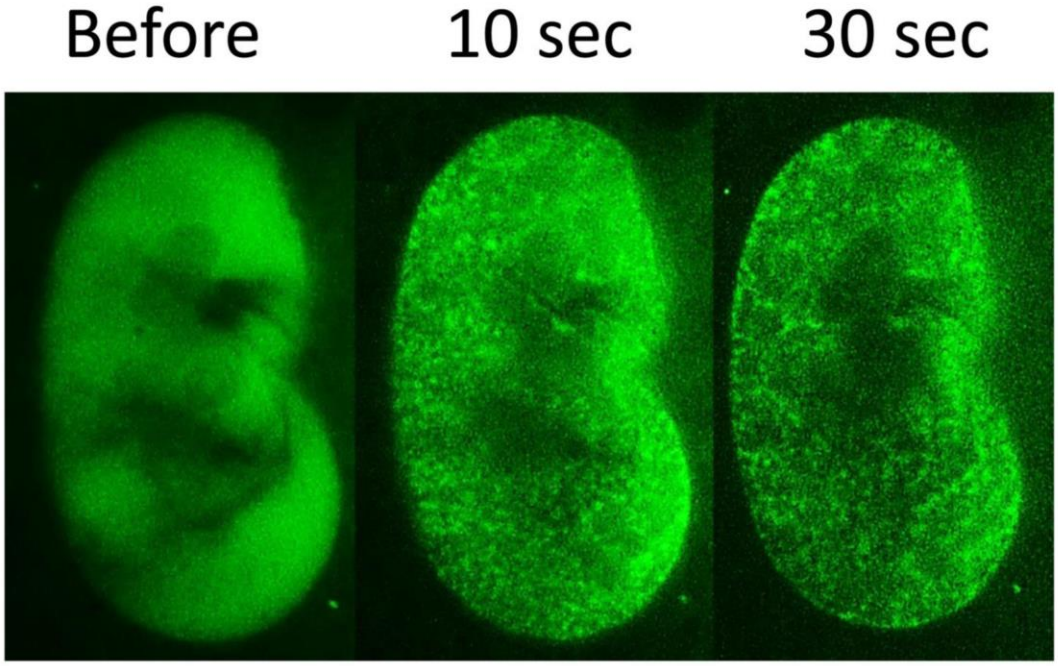

Fig. S3. Redistribution of FACT in nucleus of HT1080-treated cells from nucleoplasm to chromatin. Fluorescent imaging of the nucleus of HT1080 cells expressing GFP-tagged SSRP1 before and after treatment with 3 μM of CBL0137 for the indicated periods of time.

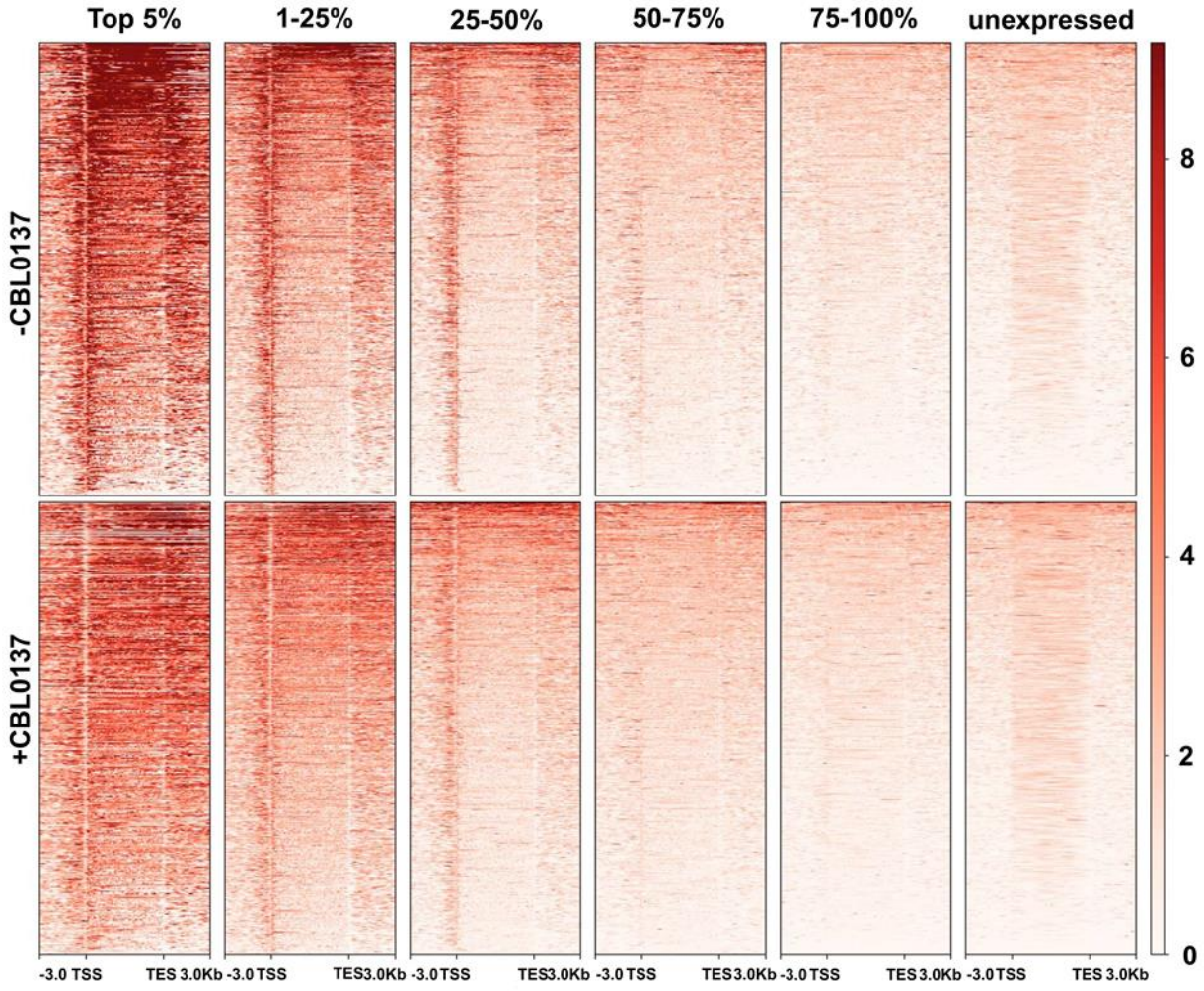

Fig. S4. Heatmaps of SSRP1 occupancy in the vicinity of TSSs and TES of the genes in HT1080 cells. The cells were incubated in the absence or in the presence of 3 μM curaxin CBL0137 for 1 hour and plotted depending on the level of transcription in control cells. SSRP1 ChIP-Seq reads are clustered based on the nascent RNA-seq data obtained in untreated HT1080 cells. The quantified data are presented in **Fig. 1C**.

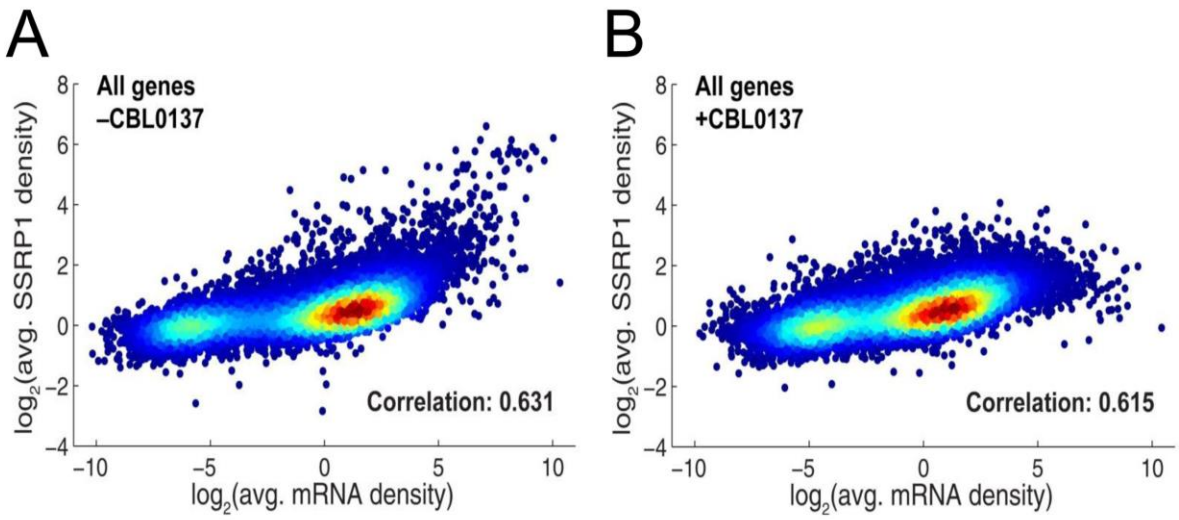

Fig. S5. Analysis of the average SSRP1 densities over gene bodies against the levels of transcription of the corresponding genes. The level of transcription of the corresponding genes is quantified by the average level of nascent transcripts determined in HT1080 cells by NET-seq. The average SSRP1 densities over gene bodies are quantified from the SSRP1 CHIP-seq data. Density scatter plots represent the analysis of all active transcribed genes in the absence (**A**) or presence (**B**) of the curaxin.

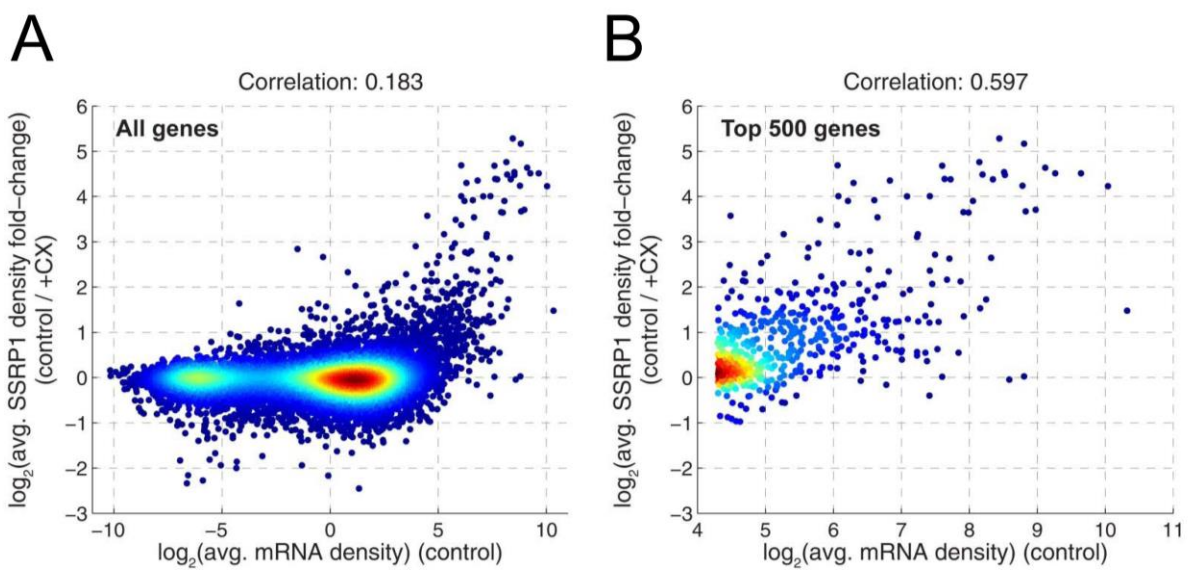

Fig. S6. Curaxins preferentially remove SSRP1 from gene bodies of highly transcribed genes. Ratio of SSRP1 density in untreated vs. CBL0137-treated cells is plotted against the nascent mRNA densities determined in HT1080 cells by NET-seq. (**A**) The change of SSRP1 density correlates with the levels of gene expression. (**B**) The correlation is enhanced in the group of top 500 most actively transcribed genes, suggesting that SSRP1 is preferentially removed from highly transcribed gene bodies in the presence of curaxins.

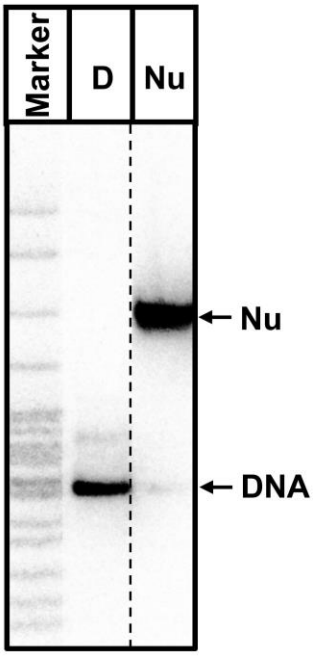

Fig. S7. Analysis of gel-purified nucleosomes by native PAGE. Marker: pBR322-*Msp*I digest. D: DNA, Nu: nucleosome.

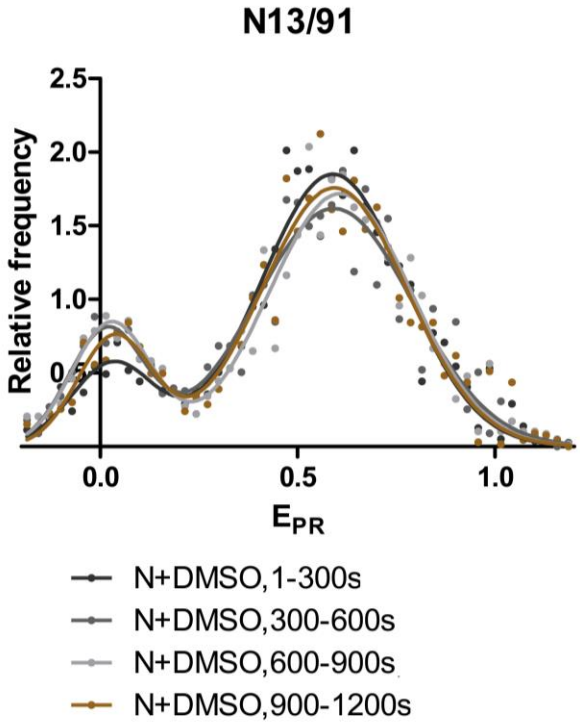

Fig. S8. Typical frequency distributions of FRET efficiencies of the N13/91 nucleosomes. Analysis by spFRET microscopy after incubations for the indicated time periods. Sample sizes (n) are shown. The distributions of E_{PR} measured during the different time intervals are similar, indicating that the majority of nucleosomes remain intact during the FRET measurements.

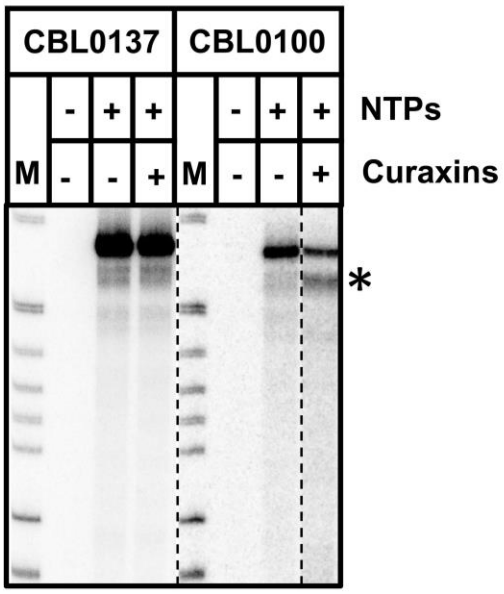

Fig. S9. The catalytic activity of Pol II is minimally affected by curaxins. The transcription of the 603 DNA template by Pol II was conducted in the presence or absence of curaxins as described in Fig. 4A. Neither CBL0137 nor CBL0100 significantly inhibit the catalytic activity of Pol II.

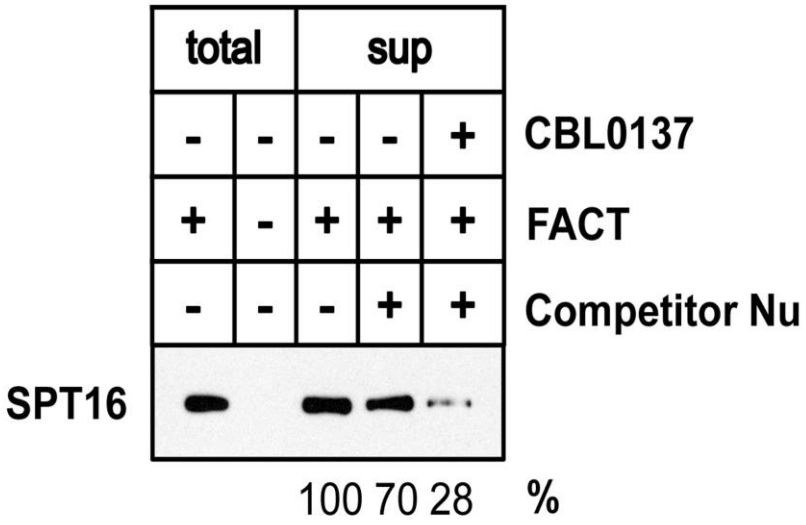

Fig. S10. Trapping of FACT on immobilized competitor nucleosomes after Pol II transcription in the presence of CBL0137. Transcription by Pol II in the presence of an excess competitor nucleosomes containing end-biotinylated DNA was conducted as described in the Fig. 4A. After transcription, the reaction mixture was fractionated using streptavidin-covered magnetic beads to immobilize biotin-labeled nucleosomes. The SPT16 protein was detected in beads-bound and supernatant fractions after separation of proteins by SDS-PAGE, blotting and immunostaining. The data were quantified using OptiQuant software and normalized for total protein loading. The amount of SPT16 in the supernatant (sup) is strongly decreased, suggesting that during transcription in the presence of CBL0137 FACT binds to biotinylated competitor nucleosomes.

Table S1. Statistical data for spFRET analysis. Mean values, amplitudes and standard deviations for spFRET distributions (calculated as a sum of two gaussians) are shown, as well as corresponding standard errors and confidence intervals.

	N,n=2510	N+CBL0137+hFACT, n=5547	N+CBL0137+hFACT+ competitor DNA, n=2566	N+CBL0137, n=1622	N+hFACT, n=6483	N+DMSO,1-300s, n=2782	N+DMSO, 300-600s, n=1950	N+DMSO, 600-900s, n=2054	N+DMSO, 900-1200s, n=2332
Best-fit values									
AMPLITUDE1	0.5532	2.368	1.16	0.9203	0.2941	0,5625	0,7871	0,8386	0,7452
MEAN1	0.02652	0.02354	0.004911	0.03472	0.01633	0,03125	0,01669	0,02782	0,03671
SD1	0.1067	0.1017	0.1025	0.09902	0.09918	0,1055	0,09661	-0,1001	-0,09467
AMPLITUDE2	1.644	0.6262	1.416	1.425	1.794	1,851	1,617	1,718	1,757
MEAN2	0.6199	0.522	0.6226	0.6033	0.6183	0,589	0,5916	0,6078	0,5927
SD2	0.2058	0.2575	0.1986	0.2168	0.2049	0,1808	0,1998	0,1813	0,1838
Std. Error									
AMPLITUDE1	0.05292	0.09256	0.06743	0.05688	0.05825	0,08025	0,09022	0,08133	0,08667
MEAN1	0.01252	0.00447	0.007092	0.007602	0.02361	0,01829	0,01342	0,01154	0,01324
SD1	0.01314	0.004924	0.007517	0.007817	0.02458	0,01919	0,01391	0,01196	0,01356
AMPLITUDE2	0.03867	0.05006	0.0486	0.03921	0.04099	0,06204	0,06362	0,06091	0,06308
MEAN2	0.005743	0.03323	0.00793	0.007204	0.005478	0,007155	0,009248	0,00748	0,007717
SD2	0.006228	0.0361	0.008363	0.007938	0.005847	0,007677	0,009928	0,007864	0,008196
95% Confidence Intervals									
AMPLITUDE1	0,4495 to 0,6569	2,187 to 2,549	1,026 to 1,295	0,8088 to 1,032	0,1800 to 0,4083	0,4006 to 0,7244	0,6050 to 0,9691	0,6745 to 1,000	0,5704 to 0,9201
MEAN1	0,001990 to 0,05105	0,01478 to 0,03230	0,0 to 0,01902	0,01982 to 0,04962	0,0 to 0,06262	0,0 to 0,0500	0,0 to 0,04376	0,004532 to 0,0500	0,01000 to 0,0500
SD1	0,08095 to 0,1325	0,09200 to 0,1113	0,08758 to 0,1175	0,08370 to 0,1143	0,05100 to 0,1474	0,06676 to 0,1442	0,06855 to 0,1247	-0,1242 to -0,07598	-0,1220 to -0,06731
AMPLITUDE2	1,568 to 1,720	0,5281 to 0,7244	1,319 to 1,513	1,348 to 1,502	1,713 to 1,874	1,725 to 1,976	1,489 to 1,745	1,595 to 1,841	1,630 to 1,885
MEAN2	0,6087 to 0,6312	0,4569 to 0,5871	0,6068 to 0,6384	0,5892 to 0,6174	0,6076 to 0,6291	0,5745 to 0,6034	0,5729 to 0,6103	0,5927 to 0,6229	0,5772 to 0,6083
SD2	0,1936 to 0,2180	0,1868 to 0,3283	0,1819 to 0,2152	0,2012 to 0,2323	0,1934 to 0,2164	0,1653 to 0,1962	0,1798 to 0,2199	0,1654 to 0,1972	0,1673 to 0,2004
Goodness of Fit									
R	0.8397	0.862	0.836	0.826	0.896	0,9306	0,8952	0,9179	0,9176